

DTIC FILE COPY

4

GL-TR-89-0319

ENVIRONMENTAL RESEARCH PAPERS, NO. 1047

Comparison of Steady State Evaporation Models for Toxic Chemical Spills: Development of a New Evaporation Model

TERI L. VOSSLER

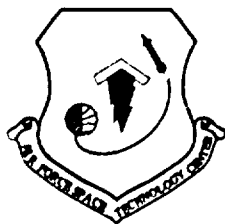
AD-A221 752



29 November 1989



Approved for public release; distribution unlimited.



DTIC
ELECTE
MAY 32 1990
S D

ATMOSPHERIC SCIENCES DIVISION

PROJECT 6670


GEOPHYSICS LABORATORY

HANSCOM AFB, MA 01731-5000

This report has been reviewed by the ESD Public Affairs Office (PA) and is releasable to the National Technical Information Service (NTIS).

"This technical report has been reviewed and is approved for publication"

FOR THE COMMANDER


DONALD D. GRANTHAM, Chief
Atmospheric Structure Branch


ROBERT A. MCCLATCHEY, Director
Atmospheric Sciences Division

Qualified requesters may obtain additional copies from the Defense Technical Information Center. All others should apply to the National Technical Information Service.

If your address has changed, or if you wish to be removed from the mailing list, or if the addressee is no longer employed by your organization, please notify GL/DAA, and GL/LYA Hanscom AFB, MA 01731-5000. This will assist us in maintaining a current mailing list.

Do not return copies of this report unless contractual obligation or notices on a specific document requires that it be returned.

REPORT DOCUMENTATION PAGEForm Approved
OMB No. 0704-0188

Public reporting for this collection of information is estimated to average 1 hour per response, including the time for reviewing instructions, searching existing data sources, gathering and maintaining the data needed, and completing and reviewing the collection of information. Send comments regarding this burden estimate or any other aspect of this collection of information, including suggestions for reducing this burden, to Washington Headquarters Services, Directorate for Information Operations and Reports, 1215 Jefferson Davis Highway, Suite 1204, Arlington, VA 22202-4302, and to the Office of Management and Budget, Paperwork Reduction Project (0704-0188), Washington, DC 20503.

1. AGENCY USE ONLY (Leave blank)		2. REPORT DATE 29 NOV 89	3. REPORT TYPE AND DATES COVERED Scientific Interim MAY 89 - NOV 89	
4. TITLE AND SUBTITLE Comparison of Steady State Evaporation Models for Toxic Chemical Spills: Development of a New Evaporation Model			5. FUNDING NUMBERS PE - 62101F PR - 6670 TA - 14 WU - 09	
6. AUTHOR(S) Teri L. Vossler*				
7. PERFORMING ORGANIZATION NAME(S) AND ADDRESS(ES) Geophysics Laboratory/LYA Hanscom AFB Massachusetts 01731-5000			8. PERFORMING ORGANIZATION REPORT NUMBER GL-TR-89-0319 ERP, No. 1047	
9. SPONSORING/MONITORING AGENCY NAME(S) AND ADDRESS(ES)			10. SPONSORING/MONITORING AGENCY REPORT NUMBER	
11. SUPPLEMENTARY NOTES Air Force Geophysics Scholar*				
12a. DISTRIBUTION/AVAILABILITY STATEMENT APPROVED FOR PUBLIC RELEASE; DISTRIBUTION UNLIMITED			12b. DISTRIBUTION CODE	
13. ABSTRACT (Maximum 200 words) The United States Air Force handles and stores a number of toxic and hazardous chemicals. Associated with this activity is the threat of accidental release. To determine the downwind threat of a spilled liquid chemical, one must estimate the evaporation rate of the spilled chemical. A steady state evaporation model is one that calculates the temperature of the spilled chemical pool based on the net energy input into the pool from all possible sources. The pool temperature is used to calculate the evaporation rate. Three steady state evaporation models are compared, and the most appropriate calculation for each energy input into the pool is identified. A new steady state evaporation model is presented based on the comparisons. Sensitivity studies are presented in support of the new model. <i>1. L. P. 1</i>				
14. SUBJECT TERMS Evaporation, toxic chemical; Spills, liquid chemical			15. NUMBER OF PAGES 56	
			16. PRICE CODE	
17. SECURITY CLASSIFICATION OF REPORT UNCLASSIFIED	18. SECURITY CLASSIFICATION OF THIS PAGE UNCLASSIFIED	19. SECURITY CLASSIFICATION OF ABSTRACT UNCLASSIFIED	20. LIMITATION OF ABSTRACT SAR	

Preface

The author gratefully acknowledges the assistance of Mr. Bruce Kunkel, who provided a careful and thoughtful review of this report and made many useful suggestions. This report was written while the author was an Air Force Geophysics Scholar, under a program administered by the Southeastern Center for Electrical Engineering Education.

Accession For	
NTIS GRA&I	<input checked="" type="checkbox"/>
DTIC TAB	<input type="checkbox"/>
Unannounced	<input type="checkbox"/>
Justification	
By _____	
Distribution/ _____	
Availability Codes	
Aval and/or	
Dist	Special
A-1	



Contents

1.	INTRODUCTION	1
2.	GENERAL DESCRIPTION OF STEADY STATE ENERGY BALANCE	3
2.1	Heat Due to Solar Radiation (Q_{sol})	3
2.1.1	SOLAR ALTITUDE ANGLE - COMPARISONS	3
2.1.2	SOLAR ALTITUDE ANGLE - RECOMMENDATION	4
2.1.3	HEAT FROM NET SOLAR RADIATION - COMPARISONS	5
2.1.4	HEAT FROM NET SOLAR RADIATION - RECOMMENDATION	6
2.2	Long Wave Radiation Emitted by the Atmosphere (Q_{atm})	7
2.2.1	COMPARISONS	7
2.2.2	RECOMMENDATION	7
2.3	Long Wave Radiation Emitted by the Pool (Q_{po})	8
2.3.1	COMPARISONS	8
2.3.2	RECOMMENDATION	8
2.4	Heat Conducted from the Ground (Q_{grd})	8
2.4.1	COMPARISONS	8
2.4.2	RECOMMENDATION	11
2.5	Heat Loss Due to Evaporation (Q_{ev})	13
2.5.1	COMPARISONS - GENERAL	13
2.5.2	MASS TRANSFER COEFFICIENT	14
2.5.3	MASS DIFFUSIVITY	15

2.5.4	RECOMMENDATIONS	17
2.6	Sensible Heat Transfer Due to Conduction and Turbulence (Q_{ht})	18
2.6.1	COMPARISONS	18
2.6.2	RECOMMENDATION	19
2.7	Evaporation Rate	20
2.8	Calculation of Liquid Chemical Pool Temperature	21
3.	SUMMARY OF THE NEW EVAPORATION MODEL	21
3.1	Heat Due to Net Solar Radiation	23
3.2	Long Wave Radiation Emitted by the Atmosphere and the Pool	24
3.3	Heat Conducted from the Ground	24
3.4	Heat Loss Due to Evaporation	26
3.5	Sensible Heat Transfer Due to Conduction and Turbulence	27
3.6	Pool Temperature Calculation	28
3.7	Chemical Data Base	29
4.	NEW MODEL SENSITIVITY STUDIES	30
4.1	Solar Altitude Angle	31
4.2	Net Heat from Solar Radiation	31
4.3	Long Wavelength Radiation Emitted by the Atmosphere	33
4.4	Long Wavelength Radiation Emitted by the Pool	34
4.5	Heat Conducted from the Ground	35
4.6	Heat Loss Due to Evaporation	36
4.6.1	PROPERTIES OF VAPOR ABOVE POOL	38
4.6.2	MASS TRANSFER COEFFICIENT	40
5.	CONCLUSIONS	43
	REFERENCES	47

Tables

1. Solar Altitude Angle from the Kawamura and MacKay (KM) Model and the ADAM Model.	4
2. Thermal Properties of Different Ground Types.	12
3. Input Data Required for Each Model.	22
4. Chemicals in New Evaporation Model Data Base.	29
5. Default Values of Parameters for Sensitivity Studies.	30
6. Effect of Solar Altitude Angle on Evaporation Rate.	31
7. Comparison of Methods for Calculating Net Heat from Solar Radiation.	32
8. Calculations for Ille and Springer Atmosphere Emissivity (0.75) vs Kawamura and MacKay Atmosphere Emissivity (0.81).	33
9. Calculations for Ille and Springer Pool Emissivity (0.95) vs Kawamura and MacKay Pool Emissivity (0.97).	34
10. Effect of Ground Type on Evaporation Rate.	35
11. ADAM Ground Heat Transfer Coefficient (ADAM h_{grd}) vs Kawamura and MacKay Ground Heat Transfer Coefficient (KM h_{grd}).	36
12. Thermal Conductivity of the Ground: Ground and Liquid Thermal Resistance vs Ground Thermal Resistance Only.	37
13. Evaporation Rates Calculated for Chemical/Air Mixture vs Air Only vs Pure Chemical Only.	38
14. Sensitivity of Pure Chemical Mole Fraction (MF) Calculation.	39
15. Sensitivity of Stability Parameter n .	40

16.	Effect of Mass Transfer Coefficient Calculation on Calculated Evaporation Rate.	41
17.	Effect of Terrain Type on Calculated Evaporation Rate.	42
18.	Effect of Wind Speed on Calculated Evaporation Rate.	42
19.	Comparison of Kawamura and MacKay Model with New Model.	43
20.	Comparison of ADAM Evaporation Model with New Model.	44
21.	Comparison of Modified Ille and Springer Model with New Model.	45

Comparison of Steady State Evaporation Models for Toxic Chemical Spills: Development of a New Evaporation Model

1. INTRODUCTION

The United States Air Force handles and stores a number of toxic and hazardous chemicals. Associated with this activity is the threat of accidental release of these dangerous chemicals. That threat applies not only to the immediate area of the spill, but to locations downwind of the spill. To determine that downwind threat, one must estimate the source strength (evaporation rate) of the spilled chemical. One spill scenario for which one must be prepared is that of a liquid chemical spilled onto the ground so that it forms a pool. To estimate the evaporation rate from the pool, data including meteorological information, properties of the spilled chemical, characteristics of the spill site, and the size of the spill, must be readily available. The procedure for estimating source strength should be simple enough to run on a microcomputer with a minimum of knowledge of the program by the user.

Several evaporation models were compared by Kunkel.¹ The Ille and Springer² model was identified as being the most realistic of the available evaporation models because it allows for

(Received for Publication 28 November 1989)

¹ Kunkel, B.A. (1983) *A Comparison of Evaporative Source Strength Models for Toxic Chemical Spills*, AFGL-TR-83-0307, ADA 139431.

² Ille, G. and Springer, C. (1978) *The Evaporation and Dispersion of Hydrazine Propellants from Ground Spills*, CEEDO-TR-78-30, ADA 059407.

changes in the pool temperature due to evaporation and solar insolation. Kunkel modified the Ille and Springer model so that it includes a parameter, n , which describes the wind velocity profile. This parameter was referred to by Kunkel as the stability index. It is a function of atmospheric stability and surface roughness. It has a significant impact on the calculated source strength. A 100 percent change in the stability index number generally results in at least a 43 percent change in the calculated evaporation rate.^{1,2} None of the other models described in the comparison by Kunkel considered the wind velocity profile. The Ille and Springer model with this change will be referred to as the modified Ille and Springer model.

Since the evaporation model comparison by Kunkel, several other evaporation models have become available which follow the same general calculation procedure as the Ille and Springer model. This procedure is a steady state balance of all sources of energy that add to or subtract from the energy of a pool of liquid which has spilled onto the ground. Each of these models takes a different approach to the calculation of each energy input. This report will serve two purposes: (1) It will compare each of three energy balance evaporation models and identify the most appropriate calculation for each energy input, and (2) it will present a new energy balance evaporation model that uses the most appropriate calculations based on the comparisons.

The models described in this report are (1) the modified Ille and Springer evaporation model,^{1,2} (2) the ADAM model liquid pool evaporation source calculation,³ (3) the Kawamura and MacKay evaporation model,⁴ and (4) the "New" evaporation model. The latter is a new model that will be recommended based on examination and evaluation of the other models.

The four models were programmed in the Basic language for the Zenith-248 microcomputer. The ADAM model is a large and complex model including many types of source strength calculations. A liquid pool evaporation model based on a steady state energy balance is included among those source calculations. The ADAM code for evaporation of a pool of liquid was extracted from the ADAM Fortran code and translated into Basic to function as a stand-alone model. The Kawamura and MacKay model was taken from its journal article description⁴ and translated into a Basic code. The modified Ille and Springer model had already been written in Basic code for the Z-248.

In Section 2, the calculation of each energy term from the modified Ille and Springer, Kawamura and MacKay, and ADAM models are evaluated. Recommendations are made for the most appropriate calculations for a new evaporation model based on evaluations. In Section 3, the new model is summarized. In Section 4, sensitivity studies are presented in support of the new model. Concluding remarks are made in Section 5.

³ Raj, P.K. and Morris, J.A. (1987) *Source Characterization and Heavy Gas Dispersion Models for Reactive Chemicals*, AFGL-TR-88-0003 (I), ADA 200121.

⁴ Kawamura, P.I. and MacKay, D. (1987) The evaporation of volatile liquids, *Journal of Hazardous Materials*, 15:343-364.

2. GENERAL DESCRIPTION OF STEADY STATE ENERGY BALANCE

The evaporation rate of a chemical from a pool surface is ultimately a function of pool surface temperature. The equilibrium surface temperature depends on many avenues of heat transfer to and from the pool. These include solar radiation (Q_{sol}), long wave radiation emitted by the pool (Q_{pol}) and the atmosphere (Q_{atm}), convective heat transfer from the atmosphere (Q_{he}), heat conducted from the ground (Q_{grd}), and heat loss due to evaporation (Q_{ev}). The steady state temperature is the temperature at which the sum of all sources of heat (energy) transported into the pool exactly balances the heat transfer out of the pool; that is, the sum of energy terms described above is zero. The steady state energy balance is expressed as:

$$Q_{sol} + Q_{atm} + Q_{pol} + Q_{he} + Q_{ev} + Q_{grd} = Q_{total} \quad (1)$$

where $Q_{total} = 0$ at steady state. Many of these energy terms can be expressed as a function of the pool surface temperature. The equation is solved iteratively for the pool temperature, which is then used to calculate evaporation rate. The evaporation rate is proportional to the mass transfer coefficient at the liquid pool - atmosphere interface and the vapor pressure of the chemical, both of which are functions of the pool surface temperature.

2.1 Heat Due to Solar Radiation (Q_{sol})

The net solar radiation reaching the spilled liquid depends on the amount of cloud cover, the time of day, and the geographical location of the pool. The last two parameters are used to calculate the solar altitude angle.

2.1.1 SOLAR ALTITUDE ANGLE - COMPARISONS

In the modified Ille and Springer model, the solar altitude angle is input by the user. This amounts to a visual estimate of the angle of the sun relative to the surface of the pool. During cloudy periods this could be difficult to do.

The ADAM model and the Kawamura and MacKay model calculate the solar altitude angle by similar methods. They both start with the following equation for the solar altitude angle, SA:

$$\sin SA = \sin LA \sin D + \cos LA \cos D \cos SHA, \quad (2)$$

where LA is the latitude, D is the solar declination, and SHA is the solar hour angle.

The models differ in their calculation of the solar declination and solar hour angle. The ADAM model follows the procedure of Woolf,⁵ which computes the exact time of meridian passage (true solar noon), needed to calculate the solar hour angle. The Kawamura and MacKay model uses the calculations given in Lunde,⁶ which sets noon equal to 12. The solar declination calculated by the Kawamura and MacKay model is likewise a simplified version of the ADAM model solar declination.

2.1.2 SOLAR ALTITUDE ANGLE - RECOMMENDATION

The Kawamura and MacKay and the ADAM models' solar altitude angle calculations are compared in Table 1. The differences between the calculated angles for the two models are trivial. Differences in solar angle as small as these are not expected to have a noticeable effect on the calculated evaporation rate. The ADAM model solar angle calculation is slightly more accurate than that of Kawamura and MacKay, yet it requires no more input information. Therefore, the ADAM model solar altitude angle calculation will be used in the new model.

Table 1. Solar Altitude Angle from the Kawamura and MacKay (KM) Model and the ADAM Model.

Date	Time	KM Solar Angle	ADAM Solar Angle
1/20	12:00	28.0	27.7
3/20	12:00	47.9	47.9
5/20	12:00	68.0	67.8
7/20	12:00	68.5	68.6
9/20	12:00	49.0	49.3
11/20	12:00	28.4	28.3
4/20	12:00	59.7	59.4
4/20	14:00	48.6	48.2
4/20	16:00	28.2	27.8
4/20	18:00	6.0	5.6
4/20	18:30	0.6	0.2
4/20	19:00	0	0
4/20	24:00	0	0

⁵ Woolf, H.M. (1980) *On the Computation of Solar Elevation Angles and the Determination of Sunrise and Sunset Times*, National Meteorological Center, Environmental Science Services Administration, Hillcrest Heights, MO.

⁶ Lunde, P.J. (1980) *Solar Thermal Engineering*, John Wiley and Sons, New York.

2.1.3 HEAT FROM NET SOLAR RADIATION - COMPARISONS

In the ADAM model, the net heat due to solar radiation is calculated as follows:

$$Q_{sol} = RS (1 - alb), \text{ Jm}^{-2}\text{s}^{-1}, \quad (3)$$

where alb is the liquid pool albedo, taken to be 0.14 (which is a standard value for water at intermediate solar angles),⁷ and RS is the net radiation per unit area reaching the pool surface. It is calculated from the following:^{8,9,10}

$$RS = \frac{990 \sin(SA) - 30}{RATl} [1 - (1 - CT) CF^{3.4}] \quad (4)$$

where SA is the solar altitude angle and RATl is the indirect radiation. CT is the cloud transmissivity (related to thickness) and CF is the fraction of sky covered by clouds. The diffuse sky radiation, RATl, is a function of solar altitude angle and is calculated from the following:

$$RATl = 0.694 + 0.00349 SA \quad \text{if } 19.4 \leq SA < 42, \text{ or} \quad (5a)$$

$$RATl = 0.49 + 0.014 SA \quad \text{if } SA < 19.4, \text{ or} \quad (5b)$$

$$RATl = 0.84 \quad \text{if } SA \geq 42. \quad (5c)$$

In the modified Ille and Springer model, the net heat due to solar radiation for a cloudless day is calculated from:

⁷ MacKay, D. and Matsugu, R.S. (1973) Evaporation rates of liquid hydrocarbon spills on land and water, *The Can. J. Ch. Eng.*, **51**:434-439.

⁸ Kunkel, B.A. (1988) *User's Guide for the Air Force Toxic Chemical Dispersion Model (AFTOX)*, AFGL-TR-88-0009, ADA 199096.

⁹ Holtslag, A.A.M. and Van Ulden, A.P. (1983) A simple scheme for daytime estimates of the surface fluxes from routine weather data, *J. Climate Appl. Meteorol.*, **22**:517-529.

¹⁰ Kasten, F. and Czeplak, G. (1980) Solar and terrestrial radiation dependent on the amount and type of cloud, *Solar Energy*, **24**:177-189.

$$Q_{sol} = \frac{1.164 \times 10^8}{RATl} (0.9^{csc SA}) (\sin SA), \text{ cal m}^{-2} \text{ hr}^{-1}. \quad (6)$$

In this equation, 1.164×10^8 ($\text{cal m}^{-2} \text{ hr}^{-1}$) represents the solar constant and 0.9 represents the transmission coefficient of the atmosphere under clear conditions. The diffuse sky radiation, RATl, is the same as in the ADAM model. If clouds are present, the type of cloud cover is input by the user (one of 8 choices ranging from cirrus to fog). Each cloud type is associated with a ratio of insolation with an overcast sky to insolation with a cloudless sky. Eq. (6) is multiplied by this ratio to get the radiation reaching the ground when clouds are present. There is no provision for taking amount of cloud cover into account.

In the Kawamura and MacKay model, the net heat calculated due to solar radiation is:

$$Q_{sol} = 4000 (1 - 0.0071 C^2) (\sin SA - 0.1), \text{ kJ m}^{-2} \text{ hr}^{-1}, \quad (7)$$

where C is the cloud cover fraction in tenths, and SA is the solar altitude angle. Note that this model does not account for the cloud thickness (transmissivity).

2.1.4 HEAT FROM NET SOLAR RADIATION - RECOMMENDATION

The solar heating equation of Kawamura and MacKay [Eq. (7)] is not valid for solar angles (SA) less than 5.74 degrees ($\sin SA < 0.1$). Q_{sol} is set equal to zero for solar angles in this range. The solar heating equation of the modified Ille and Springer model [Eq. (6)] is not valid for $SA = 0$. In those cases, SA is set equal to 1. One would expect a zero heat input due to solar radiation during the night, as calculated by the ADAM model and the Kawamura and MacKay model. The Kawamura and MacKay model does not consider cloud thickness; the modified Ille and Springer model does not consider the amount of cloud cover. The cloud type (thickness/transmissivity), as well as cloud cover, are expected to influence the solar heating.

Based on the above observations, the new model will use the ADAM model method of calculating the heat coming into the pool due to solar radiation. This method takes into account both cloud cover amount and cloud type (thickness). It calculates a value of zero for heat due to solar radiation at nighttime, and a positive value for solar altitude angles greater than zero.

2.2 Long Wave Radiation Emitted by the Atmosphere (Q_{atm})

2.2.1 COMPARISONS

The total amount of energy radiated by a black body per unit area and time is given by the Stefan-Boltzmann fourth power law:

$$E = \sigma T^4 \quad (8)$$

where T is the absolute temperature and σ is the Stefan-Boltzmann constant, $5.67 \times 10^{-8} \text{ J m}^{-2} \text{ s}^{-1} \text{ K}^{-1}$. All three of the models calculate the radiation emitted by the atmosphere using the following equation:

$$Q_{atm} = e_a \sigma T_a^4, \text{ J m}^{-2} \text{ s}^{-1}. \quad (9)$$

The additional factor e_a represents the emissivity of the atmosphere ($= 1$ for a perfect black body). e_a is a function of the water vapor pressure of the atmosphere.

The modified Ille and Springer and ADAM models set e_a equal to 0.75. The Kawamura and MacKay model calculates atmosphere emissivity via:

$$e_a = (1 - r) B, \quad (10)$$

where r is the reflectivity of the pool surface and is set equal to 0.03. B , the atmospheric radiation factor, is a function of cloud cover and vapor pressure of water in air,¹¹ and is determined graphically. A graphical determination is not practical for a computer program. In an example given by Kawamura and MacKay, the atmospheric radiation factor is equal to 0.84 at 18 mbar water vapor pressure and 20 percent cloud cover. It follows for this example that $e_a = 0.81$, compared with 0.75 assumed for the modified Ille and Springer and the ADAM models.

2.2.2 RECOMMENDATION

The calculated evaporation rate is not expected to change significantly over the range of typical atmosphere emissivities. The inconvenience of calculating the water vapor pressure and determining the atmospheric radiance factor from that, as required for the Kawamura and

¹¹ Raphael, J.M. (1962) Prediction of temperature in rivers and reservoirs, *Proc. Amer. Soc. Civ. Eng. J. Power Div.*, 88:P02.

MacKay model, is not worth the minimal benefit. Therefore, it is reasonable to assign a constant value of 0.75 to the atmosphere emissivity, as in the ADAM and the modified Ile and Springer models.

2.3 Long Wave Radiation Emitted by the Pool (Q_{pol})

2.3.1 COMPARISONS

All three of the models calculate the radiation from the pool from the Stefan-Boltzmann Law:

$$Q_{pol} = \epsilon_p \sigma T_p^4. \quad (11)$$

The emissivity of the pool (ϵ_p) is set equal to 0.95 in the modified Ile and Springer and the ADAM models, and 0.97 in the Kawamura and MacKay model. These values are approximately the emissivity of water.¹²

2.3.2 RECOMMENDATION

According to McAdams,¹² the emissivity of water for long wave radiation ranges from 0.95 to 0.963 (for temperatures ranging from 0 to 100 degrees Centigrade). For the new model, a pool of liquid with emissive properties similar to water near the freezing point will be assumed. This corresponds to an emissivity of 0.95.

2.4 Heat Conducted from the Ground (Q_{grd})

2.4.1 COMPARISONS

Heat is transferred from the ground to the liquid at the ground surface when the ground is warmer than the liquid. This heat transfer will decrease with time as the ground temperature approaches that of the liquid pool temperature. There will also be thermal resistance within the pool of liquid in transferring heat from the bottom of the liquid layer to the top, where evaporation occurs. Heat transfer from the ground to the liquid is driven by the difference in temperature between the ground and the pool:

¹² McAdams, W.H. (1954) *Heat Transmission*, 3rd edn., McGraw-Hill Book Company, Inc., New York.

$$Q_{\text{grd}} = h_g (T_g - T_p). \quad (12)$$

The modified Ille and Springer model disregards the heat transfer from the ground. It describes only the heat transfer within the liquid layer. They calculate the heat transfer coefficient from the equation:

$$h_g = \frac{k_l A Gr^B Pr^C}{L}, \text{ cal m}^{-2} \text{ hr}^{-1} \text{ K}^{-1} \quad (13)$$

where k_l = thermal conductivity of the liquid ($\text{cal m}^{-1} \text{ hr}^{-1} \text{ K}^{-1}$),

Gr = Grashof number (a function of liquid properties),

Pr = Prandtl number (a function of liquid properties),

L = depth of the liquid pool (m), and

A, B, C = constants that depend on the heat transfer mode (amount of turbulence).

The ADAM model assumes that heat transfer resistance within the liquid layer is negligible. It describes the heat transfer coefficient through the ground as follows:

$$h_g = \frac{k_g}{(\pi \alpha_g t)^{1/2}}, \text{ J m}^{-2} \text{ s}^{-1} \text{ K}^{-1}, \quad (14)$$

where k_g = thermal conductivity of the ground ($\text{J m}^{-1} \text{ s}^{-1} \text{ K}^{-1}$),

α_g = thermal diffusivity of the ground ($k_g C_{p,g} \rho_g$) ($\text{m}^2 \text{ s}^{-1}$),

t = time after spill (s),

$C_{p,g}$ = heat capacity of the ground ($\text{J kg}^{-1} \text{ K}^{-1}$), and

ρ_g = density of the ground (kg m^{-3}).

The ADAM model authors assert that the natural convective effects within the thin liquid layer are negligible compared with the heat transfer through the ground.

The Kawamura and MacKay model includes both conduction of heat from the ground and heat transfer through the liquid layer in an overall ground-liquid heat transfer coefficient, U_{grd} . It is calculated using an electrical resistance analogy:

$$U_{\text{grd}} = \frac{1}{[(1/h_g) + (1/h_l)]} \quad (15)$$

h_g is the coefficient of heat conduction through the ground, and h_l is the liquid heat transfer coefficient.

Kawamura and MacKay calculate a time-dependent heat transfer coefficient as follows:

$$h_g = \frac{2k_g}{(\pi\alpha_g t)^{1/2}} \quad (16)$$

where k_g , α_g , and t are as defined for the ADAM model.

The Kawamura and MacKay liquid heat transfer coefficient is estimated from:

$$h_l = \frac{k_l}{\phi d} \quad (17)$$

where d is the average depth of the liquid pool, approximately equal to the initial pool depth divided by 2. k_l is the liquid thermal conductivity of the liquid chemical ($\text{kJ m}^{-1} \text{ s}^{-1} \text{ K}^{-1}$), expressed as a function of pool temperature. ϕ is a liquid resistance factor for which they derive the following empirical equation:

$$\phi = 1 / \{1 + \exp[-0.06 (TB - 70)]\}, \quad (18)$$

where TB is the liquid chemical boiling point in degrees C.

2.4.2 RECOMMENDATION

In the Kawamura and MacKay model, h_g is a factor of 2 higher than the ADAM model h_g . The reference¹³ cited by Kawamura and MacKay, uses the following equation for the transient heat flow in a semi-infinite solid:

$$q_0 = \frac{-kA(T_0 - T_1)}{(\pi\alpha_g t)^{1/2}} \quad (19)$$

where q_0 = heat transfer rate at the solid surface, $J s^{-1}$,

k = thermal conductivity of the ground, $kJ m^{-1} s^{-1} C^{-1}$,

A = area, m^2 ,

$\alpha_g = k \rho C$ = thermal diffusivity of the ground, $m^2 s^{-1}$,

ρ = density, $kg m^{-3}$,

C = specific heat capacity, $kJ kg^{-1} C^{-1}$,

t = time constant, s ,

T_0 = surface temperature of the ground, and

T_1 = initial temperature of the bulk ground.

A number of other references provide a similar analysis of the time-dependent heat flow in a semi-infinite solid.^{14,15} Therefore, the new evaporation model will describe the time-dependent heat transfer coefficient as derived in the aforementioned references. This is the same calculation as in the ADAM model.

Both the ADAM and Kawamura and MacKay models assume constant values for the ground properties. But those properties can vary substantially depending on the type of soil or surface on which the chemical has spilled. Table 2 lists various ground types and their corresponding thermal conductivities and thermal diffusivities. In the new model, an option will be added whereby the user can choose the type of soil or surface on which the chemical has spilled.

¹³ Holman, J.P. (1976) *Heat Transfer*, 4th edn., McGraw-Hill Book Company, Inc., New York.

¹⁴ Bird, R.B., Stewart, W.E., and Lightfoot, E.N. (1960) *Transport Phenomena*, John Wiley and Sons, Inc., New York.

¹⁵ Schneider, P.J. (1955) *Conduction Heat Transfer*, Addison-Wesley Publishing Co., Cambridge, MA.

Table 2. Thermal Properties of Different Ground Types.

Soil/Surface Type	Thermal Conductivity $\text{W m}^{-1} \text{K}^{-1}$	Thermal Conductivity Reference	Diffusivity m^2/s	Diffusivity Reference
Dry Soil	0.138	16	1.1×10^{-7}	*
Wet Soil	0.657	17	1.9×10^{-7}	17
Dry Sand	0.326	17	2.74×10^{-6}	17
Wet Sand	1.128	17	4.92×10^{-6}	17
Concrete	1.279	17	4.92×10^{-6}	17

*Estimated from $\alpha = k/(\rho C_p)$ for soil organic matter.

As shown in the example below, the thermal resistance of the liquid as calculated by the Kawamura and MacKay method is non-negligible compared with the ground heat conduction.

Example

Let chemical = N_2O_4 (TB = 21.2, C)

$t = 10 \text{ min} = 600 \text{ s}$

$k_g = 0.657 \text{ W m}^{-1} \text{K}^{-1}$ (wet soil)

$\alpha_g = 1.9 \times 10^{-7}$ (wet soil)

$h_g = 0.657 / (\pi \times 1.9 \times 10^{-7} \times 600)^{1/2} = 34.7 \text{ W m}^{-2} \text{K}^{-1}$

$d = 0.5 \text{ cm} = 0.005 \text{ m}$ (average pool depth)

$\phi = 1/(1 + \exp[-0.06(21.2 - 70)]) = 0.05076$

$k_l = 0.132 \text{ W m}^{-1} \text{K}^{-1}$

therefore, $h_l = 520 \text{ W m}^{-2} \text{K}^{-1}$ and $U_{\text{grd}} = 32.6 \text{ W m}^{-2} \text{K}^{-1}$.

The overall ground/liquid heat conduction is 7 percent lower than the heat conduction from the ground only. For a deeper pool, the reduction in the ground heat conduction by the liquid is even greater. For instance, a pool whose initial depth is equal to 5 cm has a liquid thermal resistance that lowers the overall ground/liquid heat conduction by 25 percent. It is expected that a change in ground heat conduction of this magnitude can have some effect on the calculated evaporation rate.

¹⁶ Dean, J.A. (1985) ed. *Lange's Handbook of Chemistry*, 13th edn., McGraw-Hill Book Company, New York.

¹⁷ Kothandaraman, C.P. and Subramanyan, S. (1975) *Heat and Mass Transfer Data Book*, 2nd edn., John Wiley and Sons, New York.

The overall procedure suggested by Kawamura and MacKay for calculating the heat conducted through the ground and liquid pool will be used in the new model, with the elimination of the factor of 2 in Eq. (16). This procedure allows pool depth to be selected (rather than assigned a constant value, as in the ADAM model) and takes into account heat transferred through both the ground and the liquid. Eq. (12) then becomes:

$$Q_{\text{grd}} = U_{\text{grd}} (T_g - T_p) \quad \text{J m}^{-2} \text{s}^{-1}. \quad (20)$$

2.5 Heat Loss Due to Evaporation (Q_{ev})

2.5.1 COMPARISONS - GENERAL

Vapor transfer from the surface of the pool to the surrounding atmosphere is governed by the mass transfer coefficient and the concentration gradient between the vapor at its source and in the ambient surroundings:

$$E = k_m (C_p - C_a), \text{ kg m}^{-2} \text{s}^{-1}. \quad (21)$$

E is the mass evaporation rate per unit area, k_m is the mass transfer coefficient (m/s) and C_p and C_a are the vapor concentrations at the pool surface/air interface and in the surrounding air, respectively. Assuming $C_a = 0$ and the vapor behaves as an ideal gas, one can write

$$E = \frac{k_m M P_{\text{sat}}}{RT_p}, \text{ kg m}^{-2} \text{s}^{-1}, \quad (22)$$

where M (kg/mol) is the vapor molecular weight, P_{sat} is its saturation vapor pressure (Pa), R is the ideal gas constant ($\text{J mol}^{-1} \text{K}^{-1}$), and T_p is the absolute temperature of the pool. The rate of heat loss due to evaporation per unit area is the product of the evaporation rate and the heat of vaporization, H_v (J/kg):

$$Q_{\text{ev}} = E H_v = k_m \frac{M P_{\text{sat}}}{RT} H_v, \text{ W m}^{-2}. \quad (23)$$

2.5.2 MASS TRANSFER COEFFICIENT

All the models discussed here use this same general procedure for calculating the evaporative cooling of a pool of liquid. They differ in the calculation of the mass transfer coefficient. Mass transfer is a fundamental property important to the evaporation process. It is therefore important to understand the details of the calculation of this property.

In the modified Ille and Springer model, the mass transfer coefficient is calculated in terms of the wind speed, U (m/h), and pool diameter, X (m) (or more precisely, the distance across the pool in the downwind direction), as given by Sutton:¹⁸

$$k_m = 0.0292 Sc^{-0.667} U^{\frac{2-n}{2+n}} X^{\frac{-n}{2+n}}, \text{ m/hr.} \quad (24)$$

Sc is the Schmidt number, a dimensionless number calculated by dividing the kinematic viscosity of the air/chemical vapor mixture by the diffusivity of the chemical vapor in the air. Mass diffusivity, like mass transfer, is calculated differently by each evaporation model. This will be discussed later in this section. The constant n is chosen to describe the wind velocity profile. It is a function of the terrain roughness and the atmospheric stability (solar altitude angle, cloud cover, and wind speed) and is a very sensitive parameter. n has been estimated by Sinedman-Hogstrom and Hogstrom.¹⁹ Ille and Springer show that a 100 percent change in n results in a 43 percent or greater change in the evaporation rate.

The Kawamura and MacKay model calculates mass transfer coefficient in basically the same way as the modified Ille and Springer model, but with a few simplifications. Rather than selecting n based on terrain type and atmospheric stability, the model chooses a constant value of 0.25 for n to represent typical atmospheric and terrain conditions. This is the same calculation as the original Ille and Springer model. Mass transfer coefficient then becomes:

$$k_m = 0.0292 Sc^{-0.667} U^{0.78} X^{-0.11}. \quad (25)$$

¹⁸ Sutton, O.G. (1953) *Micrometeorology*, McGraw-Hill Book Company, Inc., New York.

¹⁹ Sinedman-Hogstrom, A.S. and Hogstrom, U. (1978) A practical method for determining wind frequency distribution for the lowest 200 m from routine meteorological data, *J. of Appl. Meteorol.*, 17:942-954.

The ADAM model calculates the mass transfer coefficient as:

$$k_m = \frac{\mu_m}{X} \frac{0.037}{Sc^{0.617}} (Re^{0.8} - 15,500), \text{ m/s}, \quad (26)$$

where μ_m is the kinematic viscosity of the pure chemical vapor, X is the pool diameter, Sc is the Schmidt number (as defined previously), and Re is the Reynolds number. Re is calculated from the wind speed, pool width, and viscosity by:

$$Re = \frac{UX}{\mu_m}, \quad (27)$$

The ADAM model uses the kinematic viscosity of the pure chemical vapor to calculate the Schmidt number. The Kawamura and Mackay model uses the kinematic viscosity of the air, and the modified Ilie and Springer model uses the kinematic viscosity of the chemical vapor/air mixture. The Kawamura and Mackay model also simplifies the Schmidt number by setting it equal to the kinematic viscosity of the air (rather than the chemical/air mixture) divided by the diffusivity of the chemical in air.

2.5.3 MASS DIFFUSIVITY

As with the overall mass transfer, the models differ in their approach to the mass diffusivity. The modified Ilie and Springer model uses an estimation method for diffusivity based on theory:

$$DV_{ab} = \frac{0.00266 T^{3/2}}{P M_{ab}^{1/2} \sigma_{ab}^2 \Omega_D}, \text{ cm}^2/\text{s}, \quad (28)$$

where

DV_{ab} = molecular diffusion coefficient of chemical a in chemical b,

$$M_{ab} = 2 \left[\frac{1}{M_a} + \frac{1}{M_b} \right]^{-1}, \quad (29)$$

M_a, M_b = molecular weights of a and b,

σ = characteristic length (\AA) = $(\sigma_a + \sigma_b)/2$,

Ω_D = diffusion collision integral.

The characteristic length and collision integrals are calculated from the following:

$$\sigma = 1.18 V_b^{1/3} \quad (V_b = \text{liquid volume at boiling point}), \quad (30)$$

$$\Omega_D = 10^{(-0.43 \log(T_p)/2.303 + \text{OMECK})}, \quad (31)$$

OMECK is the collision integral constant, unique to each chemical and not widely available.

T_p is the temperature of the pool of liquid.

Kawamura and Mackay used data from Holman¹⁹ for the molecular diffusion coefficient in the example that they gave. This value was given for a specific temperature as opposed to calculating it for each temperature iteration.

The ADAM model uses the method of Fuller et al^{20,21,22} to calculate the molecular diffusion coefficient:

$$DV_{ab} = \frac{0.00143 T^{1.75}}{P M_{ab}^{1/2} \left[(\Sigma_v)_a^{1/3} + (\Sigma_v)_b^{1/3} \right]^2}, \quad (32)$$

²⁰ Fuller, E.N. and Giddings, J.C. (1965) A comparison of methods for predicting gaseous diffusion coefficients, *J. Gas Chromatogr.*, 3:222-227.

²¹ Fuller, E.N., Emsley, K., and Giddings, J.C. (1969) Diffusion of halogenated hydrocarbons in helium: The effect of structure on collision cross sections, *J. Phys. Chem.*, 73:3679-3685.

²² Fuller, E.N., Schlettler, P.D., and Giddings, J.C. (1966) A new method for prediction of binary gas-phase diffusion coefficients, *Ind. Eng. Chem.*, 58:18-27.

where the Σ_v 's are the molecular diffusion volumes. The other parameters have been previously identified. Atmospheric pressure, P , is in units of bars.

2.5.4 RECOMMENDATIONS

The heat loss due to evaporation for the three models discussed differs essentially in the calculation of the molecular diffusion and mass transfer at the interface of the liquid pool and the atmosphere. A recommendation of the most appropriate evaporative cooling calculation should then focus on the best mass transfer and diffusivity calculation.

The modified Ille and Springer mass transfer coefficient calculation is the only one that attempts to estimate the wind profile, based on the time of day, cloud cover, and terrain roughness. These parameters strongly influence the mass transfer coefficient, and thus the evaporation rate and evaporative heat loss. Intuitively, one would expect parameters such as terrain roughness and amount of sunlight to affect the wind profile, and thus the mass transfer rate.

The Schmidt number is a fundamental component of the mass transfer coefficient. The Schmidt number is a dimensionless parameter calculated from the kinematic viscosity and molecular diffusivity. Viscosity can be estimated for pure air, pure chemical vapor, or a chemical vapor/air mixture. While air properties may be sufficient for a very low chemical vapor pressure and pure chemical properties sufficient for a nearly atmospheric pressure of the vapor, one does not know *a priori* which situation will prevail. Furthermore, comparable amounts of air and chemical vapor may exist at the liquid pool/air interface. Therefore, it is best to calculate the kinematic viscosity of the chemical vapor/air mixture. Kinematic viscosity, μ , is obtained from the dynamic viscosity, η , and the vapor density, ρ_v via $\mu = \eta/\rho_v$. The dynamic viscosity of air and some pure chemical vapors can be found in the literature, usually as functions of the temperature of the vapor.

The properties of a mixture are calculated from the average molar fraction, MF , of the pure chemical in the mixture. In the modified Ille and Springer model the average molar fraction is approximately 1/2 times the ratio of the chemical saturation vapor pressure to the atmospheric pressure.

The viscosity of the chemical/air mixture is calculated from:²³

$$\eta_{mix} = \frac{MF MW \eta_{ch} + (1 - MF) MWA \eta_{air}}{MF MW^{1/2} + (1 - MF) MWA^{1/2}}, \quad (33)$$

where MW = molecular weight of the chemical, and
 MWA = molecular weight of the air.

²³ Perry, R.H., and Chilton, C.H., eds. (1973) *Chemical Engineers' Handbook*, 5th edn., McGraw-Hill Book Company, Inc., New York.

The vapor density of the mixture, $\rho_{v,mix}$ is calculated from:

$$\rho_{v,mix} = \frac{[MF MW + MWA (1 - MF)] P_{atm}}{R T}, \quad (34)$$

where all quantities are as defined previously.

Molecular diffusivity is another fundamental property of the evaporating liquid pool. There have been many methods proposed for calculating diffusivity in a low pressure binary gas system, both empirical and theoretical. An important requirement of an evaporation model is that input data be obtainable. Reid et al²⁴ reviewed several calculations and identified the method of Fuller et al^{20,21,22} as the one yielding the smallest average error. The method of Fuller et al was described by Eq. (32). The molecular diffusion volumes can be obtained by summing the appropriate atomic diffusion volumes listed on page 588 of Reid et al.²⁴ The other parameters, identified previously, are easily obtainable. Therefore, the Fuller et al diffusivity calculation is recommended for the new evaporation model.

In summary, the new evaporation model will calculate the evaporative cooling via Eq. (22). The mass transfer coefficient calculation of Ilie and Springer will be adopted. Viscosity and vapor density of the chemical vapor mixture and the molecular diffusivity of Fuller et al will be used to calculate the dimensionless Schmidt number.

2.6 Sensible Heat Transfer Due to Conduction and Turbulence (Q_h)

2.6.1 COMPARISONS

The rate of transfer of sensible heat per unit area by air flowing over the uniformly heated pool surface is driven by the temperature difference between the air and the chemical pool:

$$Q_h = k_h (T_a - T_p), W/m^2. \quad (35)$$

T_a and T_p are the temperature of the atmosphere and the pool, respectively, and k_h is the heat transfer coefficient. The heat and mass transfer coefficients are related by:

²⁴ Reid, R.C., Prausnitz, J.M., and Poling, B.E. (1987) *The Properties of Gases and Liquids*, 4th edn., McGraw-Hill Book Company, Inc., New York.

$$k_h = k_m \rho_v C_{p,v} (Sc/Pr)^{0.667}, \text{ J m}^{-2} \text{ s}^{-1} \text{ K}^{-1}. \quad (36)$$

The mass transfer coefficient (k_m), vapor density (ρ_v), and Schmidt number have been defined previously. $C_{p,v}$ is the vapor heat capacity at constant pressure. Pr is the Prandtl number, a dimensionless heat transfer parameter defined as:

$$Pr = \frac{C_{p,v} \eta_v}{TCONV}, \quad (37)$$

where $C_{p,v}$ ($\text{J kg}^{-1} \text{ K}^{-1}$) and η_v ($\text{kg m}^{-1} \text{ s}^{-1}$) are the vapor heat capacity and dynamic viscosity, respectively. $TCONV$ is the vapor thermal conductivity ($\text{J m}^{-1} \text{ s}^{-1} \text{ K}^{-1}$).

The three models use the same general procedure to calculate the net heat transfer due to conduction and turbulence. However, their heat transfer coefficients differ, just as their mass transfer coefficients differ. Differences in mass transfer coefficient and Schmidt number have been described and recommendations made (Section 2.5). The remaining differences are in thermodynamic properties of the vapor, namely, heat capacity, density, viscosity, and thermal conductivity.

In the modified Ille and Springer model, thermodynamic properties are calculated for the mixture of chemical vapor and air at the interface of the atmosphere and the pool. The ADAM model uses properties of the pure chemical vapor only, while the Kawamura and MacKay model uses properties of the air only. Furthermore, the ADAM and the modified Ille and Springer models calculate properties as functions of temperature, while the Kawamura and MacKay model uses constant values of air properties.

2.6.2 RECOMMENDATION

The heat transfer due to conduction and turbulence is described by Eqs. (35) and (36). The three models discussed differ in their treatment of the mass transfer process and thermodynamic properties. These topics were discussed in Section 2.5. As concluded in Section 2.5, one does not know *a priori* whether air or pure chemical will dominate the vapor above the liquid pool. For this reason, the new evaporation model follows the modified Ille and Springer model by calculating the thermodynamic properties of the chemical vapor/air mixture.

A method was given for calculating the viscosity of a mixture in Section 2.5. The thermal conductivity, heat capacity, and density of the vapor should likewise be calculated for the chemical vapor/air mixture. A method for calculating the vapor density of a mixture was

given in Eq. (34). The thermal conductivity of the chemical vapor/air mixture is calculated from Eq. (38), given in Reference 23:

$$TCONVMIX = \frac{MF TCONV MW^{1/3} + (1 - MF) MWA^{1/3} TCONVA}{MF MW^{1/3} + (1 - MF) MWA^{1/3}}, \quad (38)$$

where $TCONV$ = thermal conductivity of the pure chemical vapor, calculated as a function of temperature,
 $TCONVA$ = thermal conductivity of air (set equal to a constant), and
 $TCONVMIX$ = thermal conductivity of the mixture.

MF, MW, and MWA were defined previously.

The heat capacity of a mixture is calculated by simple averaging:

$$C_{p,mix} = \frac{MF C_{p,v} MW + (1 - MF) C_{p,a} MWA}{MF MW + (1 - MF) MWA}, \quad (39)$$

$C_{p,mix}$ = heat capacity of the mixture,
 $C_{p,v}$ = heat capacity of pure chemical vapor, calculated as a function of temperature, and
 $C_{p,a}$ = heat capacity of the air, given as a constant value.

In summary, the new evaporation model will calculate the heat transfer due to conduction and turbulence via Eqs. (35) and (36). The mass transfer coefficient calculation of modified Ille and Springer will be adopted. Viscosity, vapor density, thermal conductivity, and heat capacity will be calculated for the chemical vapor/air mixture at the pool/atmosphere interface. The molecular diffusivity will be calculated by the method given in Eq. (32).

2.7 Evaporation Rate

The mass evaporation rate per unit area, E , is calculated assuming the vapor at the pool surface/air interface behaves as an ideal gas:

$$E = \frac{k_m M P_{sat}}{R T_p}, \text{ kg m}^{-2} \text{ s}^{-1}. \quad (40)$$

k_m , the mass transfer coefficient (m/s), is calculated as in Eq. (24) and is a function of pool temperature, T_p . The saturation vapor pressure of the chemical, P_{sat} (Pa), is also a function of the pool temperature via the Antoine equation:¹⁸

$$\log P_{sat} = A - \frac{B}{C + T_p}, \quad (41)$$

where A, B, and C are constants unique to each chemical.

To get the overall evaporation rate in kg/s, Eq. (40) is multiplied by the surface area, A, of the pool. In the modified Ille and Springer and the Kawamura and MacKay models, the area is input by the user. In the ADAM model it is calculated from the volume of chemical spilled, assuming a pool depth of 1 cm.

2.8 Calculation of Liquid Chemical Pool Temperature

Many of the energy terms comprising Eq. (1), the steady state energy balance, can be expressed as functions of the pool temperature. The evaporation models solve for the pool temperature using the Newton-Raphson iterative procedure.

3. SUMMARY OF THE NEW EVAPORATION MODEL

In the previous section, three steady state energy balance evaporation models for a pool of spilled liquid chemical were compared and evaluated. A new evaporation model was proposed based on these evaluations. In this section, a summary of the new evaporation model is presented. The new model is a composite of the three models reviewed in Section 2.

Table 3 shows the input data required for each model.

Table 3. Input Data Required for each Model.

Physical Data	I&S	ADAM	K&M	New
Location (latitude, longitude)	X	X	X	X
Date (month, day)		X	X	X
Time of Day		X	X	X
Time Since Spill			X	X
Air Temperature	X	X	X	X
Ground Temperature	X	X	X	X
Chemical Storage Temperature	X	X		X
Wind Speed	X	X	X	X
Atmospheric Pressure (can assume 1 atm)	X	X	X	X
Solar Angle	X	calc.	calc.	calc.
Spill Area/Diameter	X	calc.	X	calc.
Spill Depth	X	given	X	X
Terrain Type	X			X
Ground Type			given	X
Volume Chemical Spilled		X	X	X
Cloud Cover Fraction	X	X	X	X
Cloud Thickness	X	X		X
Relative Humidity			X	
Chemical Data				
Molecular Weight Chemical	X	X	X	X
Molecular Weight Air	X	X	X	X
Molecular Diffusion Volume Chemical		calc.		X
Molecular Diffusion Volume Air		X		X
Ground Heat Capacity		X	X	X
Ground Thermal Diffusivity		X	X	X
Vapor Pressure of Chemical	X	X	X	X
Vapor Pressure of Water			X	
Diffusivity of Chemical in Air	calc.	calc.		calc.
Liquid Density of Chemical	X			
Liquid Thermal Conductivity of Chemical	X		X	X
Liquid Heat Capacity of Chemical	X			
Liquid Viscosity of Chemical	X			
Vapor Heat Capacity of Chemical	X	X		X
Vapor Heat Capacity of Air	X		X	X
Vapor Viscosity of Chemical	X	X		X
Vapor Viscosity of Air	X		X	X
Vapor Thermal Conductivity of Chemical	X	X		X
Vapor Thermal Conductivity of Air	X		X	X
Boiling Point of Chemical	X	X	X	X
Freezing Point of Chemical		X		X
Enthalpy of Vaporization of Chemical	X	X	X	X
Critical Temperature	X			
Grashof Number	calc.			
Prandtl Number	calc.	calc.	X	calc.
Collision Integral	X			
Effective Diameter	X			

These data are supplied by separate chemical data files and by user input during program execution. The modified Ille and Springer model and the new model require the most chemical data. Unavailability of chemical data may limit the use of these models.

All of the models reviewed and the one proposed are steady state energy balance evaporation models. A steady state energy balance evaporation model is one in which the sum of all sources of energy (heat) transported into the pool exactly balances the sum of energy sources transported out of the pool. Many of these sources of energy can be expressed in terms of the liquid chemical pool temperature, which is calculated iteratively. That calculated temperature is used to calculate the evaporation rate.

The steady state energy balance is expressed as:

$$Q_{sol} + Q_{atm} + Q_{pol} + Q_{he} + Q_{ev} + Q_{grd} = 0. \quad (42)$$

Terms of this equation were defined in Section 1 and described in detail in Section 2. Calculations for the new model are summarized below.

3.1 Heat Due to Net Solar Radiation

The net heat due to solar radiation reaching the spilled liquid depends on the angle of the sun with respect to the pool and the amount and type of cloud cover. The solar altitude angle, SA, is calculated using an equation from Reference 5:

$$\sin SA = \sin LA \sin D + \cos LA \cos D \cos SHA. \quad (43)$$

LA is the geographical latitude of the pool, D is the solar declination, and SHA is the solar hour angle.

The heat from the net solar radiation is calculated as in the ADAM model:

$$Q_{sol} = RS (1 - alb), W/m^2. \quad (44)$$

The liquid pool albedo, alb, is included to correct for solar radiation reflected away from the pool. The net radiation per unit area, RS, is calculated from the following:^{8,9,10}

$$RS = \frac{990 \sin(SA) - 30}{RATI} (1 - (1 - CT) CF^{3.4}) \quad (45)$$

where SA is the solar altitude angle and RATI is the diffuse sky radiation. CT is the cloud transmissivity (related to thickness) and CF is the fraction of sky covered by clouds. The diffuse sky radiation, RATI, is a function of solar altitude angle and is calculated from:

$$RATI = 0.694 + 0.00349 SA \quad \text{if } 19.4 \leq SA < 42, \text{ or} \quad (46a)$$

$$RATI = 0.49 + 0.014 SA \quad \text{if } SA < 19.4, \text{ or} \quad (46b)$$

$$RATI = 0.84 \quad \text{if } SA \geq 42. \quad (46c)$$

3.2 Long Wave Radiation Emitted by the Atmosphere and the Pool

The long wavelength radiation emitted by the atmosphere, Q_{atm} , and the liquid pool, Q_{pol} , is calculated from the Stefan-Boltzmann law:

$$Q_{atm} - Q_{pol} = \epsilon_a \sigma T_a^4 - \epsilon_p \sigma T_p^4, \text{ W/m}^2. \quad (47)$$

The emissivity of the atmosphere and the pool, ϵ_a and ϵ_p , are set equal to 0.75 and 0.95, respectively. The Stefan-Boltzmann constant σ is equal to $5.67 \times 10^{-8} \text{ W m}^{-2} \text{ K}^{-4}$. T_a and T_p are the air and pool temperatures. The former is input by the user while the latter is calculated iteratively. Q_{pol} is negative because heat is leaving the chemical pool.

3.3 Heat Conducted from the Ground

Heat is transferred from the ground to the liquid at the ground surface. There is also a thermal resistance within the pool of liquid in transferring heat from the bottom of the liquid layer to the top, where evaporation occurs. In the new model, heat conduction through the ground and heat transfer through the liquid layer are combined in an overall ground heat transfer coefficient:

$$U_{\text{grd}} = \frac{1}{[(1/h_g) + (1/h_l)]}, \text{ W m}^{-1} \text{ K}^{-1}, \quad (48)$$

where h_g is the coefficient of heat conduction through the ground, and h_l is the liquid heat transfer coefficient.

The heat transfer coefficient through the ground is calculated using an equation from Reference 13:

$$h_g = \frac{k_g}{(\pi \alpha_g t)^{1/2}}, \text{ J m}^{-2} \text{ s}^{-1} \text{ K}^{-1}, \quad (49)$$

where k_g = thermal conductivity of the ground ($\text{J m}^{-1} \text{ s}^{-1} \text{ K}^{-1}$),

α_g = thermal diffusivity of the ground ($\text{m}^2 \text{ s}^{-1}$), and t = time after spill (s).

The user is asked to choose the type of soil or surface best describing that on which the chemical has spilled. The choices are dry soil, wet soil, dry sand, wet sand, or concrete. The model includes values for thermal conductivity and thermal diffusivity as given in Table 2 for each of the ground types. The time parameter is input by the user.

The liquid heat transfer coefficient will be estimated by the method of Kawamura and MacKay:⁴

$$h_l = \frac{k_l}{\phi d}, \text{ W m}^{-2} \text{ K}^{-1}. \quad (50)$$

The liquid thermal conductivity, k_l , is expressed as a function of pool temperature. The initial depth of the pool, d , is input by the user. The model uses the average pool depth, which is estimated to be one half times the initial pool depth. Kawamura and MacKay have derived the following empirical equation⁴ for the liquid resistance factor ϕ :

$$\phi = 1 / \{1 + \exp[-0.06 (TB - 70)]\}. \quad (51)$$

where TB is the chemical boiling point in degrees C.

3.4 Heat Loss Due to Evaporation

The evaporation rate of the liquid chemical from the pool can be described by the equation:

$$E = \frac{k_m M P_{sat}}{R T_p}, \text{ kg m}^{-2} \text{ s}^{-1}, \quad (52)$$

where k is the mass transfer coefficient, M is the vapor molecular weight (kg/mole), P_{sat} is its saturation vapor pressure (Pa), R is the ideal gas constant ($\text{J mol}^{-1} \text{ K}^{-1}$), and T_p is the absolute temperature of the pool. The rate of heat loss due to evaporation per unit area is the product of the evaporation rate and the heat of vaporization, H_v :

$$Q_{ev} = -E H_v = -k_m \frac{M P_{sat}}{R T_p} H_v, \text{ W m}^{-2}, \quad (53)$$

The heat of vaporization, H_v , is calculated as a function of temperature of the pool.

The mass transfer coefficient k_m is calculated from the method of Sutton,¹⁸ as in the modified Ille and Springer model:

$$k_m = 0.0292 \text{ Sc}^{-0.667} U^{\frac{2-n}{2+n}} X^{\frac{-n}{2+n}}, \text{ m/hr.} \quad (54)$$

U (m/h) is the wind speed at the spill site and X (m) is the pool diameter (width in downwind direction). The mass transfer coefficient units are converted to m/s by dividing by 3600.

The Schmidt number, Sc , is a dimensionless number calculated by dividing the kinematic viscosity, μ , of the air/chemical vapor mixture by the diffusivity, DV_{ab} , of the chemical vapor in the air:

$$Sc = \frac{\mu}{DV_{ab}} = \frac{\eta}{\rho_v DV_{ab}}, \quad (55)$$

η is the dynamic viscosity of the vapor mixture and ρ_v is the density of the vapor mixture.

The mass diffusivity of the chemical vapor in air is calculated by the method of Fuller et al.^{20,21,22}

$$DV_{ab} = \frac{0.00143 T_P^{1.75}}{P M_{ab}^{1/2} \left[(\Sigma_v)_a^{1/3} + (\Sigma_v)_b^{1/3} \right]^2}, \text{ cm}^2/\text{s}. \quad (56)$$

The Σ_v 's are the molecular diffusion volumes. These can be obtained by summing the appropriate atomic diffusion volumes listed on page 588 of Reid et al.²³ The other parameters, identified previously, are easily obtainable. Atmospheric pressure, P , is in units of bars.

The constant n in Eq. (54) describes the wind velocity profile. It is a function of the terrain roughness and the atmospheric stability (solar altitude angle, cloud cover, and wind speed) and is a very sensitive parameter. Smedman-Hogstrom and Hogstrom¹⁹ have estimated n .

3.5 Sensible Heat Transfer Due to Conduction and Turbulence

The rate of transfer of sensible heat per unit area by air flowing over the uniformly heated pool surface is driven by the temperature difference between the air and the chemical pool:

$$\dot{Q}_{he} = k_h (T_a - T_p), \text{ W/m}^2. \quad (57)$$

T_a and T_p are the temperature of the atmosphere and the pool, respectively, and k_h is the heat transfer coefficient. The heat and mass transfer coefficients are related by:

$$k_h = k_m \rho_v C_{p,v} (Sc/Pr)^{0.667}, \text{ J m}^{-2} \text{ s}^{-1} \text{ K}^{-1}. \quad (58)$$

The mass transfer coefficient (k_m), vapor density (ρ_v), and Schmidt number have been defined previously. $C_{p,v}$ is the vapor heat capacity at constant pressure of the air/chemical mixture. It is calculated as a function of pool temperature. Pr is the Prandtl number, a dimensionless heat transfer parameter defined as follows:

$$Pr = \frac{C_{p,v} \eta_v}{TCONV}, \quad (59)$$

where $C_{p,v}$ ($J\ kg^{-1}\ K^{-1}$) and η_v ($kg\ m^{-1}\ s^{-1}$) are the vapor heat capacity and dynamic viscosity, respectively. T_{CONV} is the vapor thermal conductivity ($J\ m^{-1}\ s^{-1}\ K^{-1}$). Each of these thermodynamic parameters is a function of the pool temperature.

Note that when the pool is warmer than the air there will be a loss of heat from the pool by this heat transfer mode, and the calculated sensible heat flux into the pool will be negative.

3.6 Pool Temperature Calculation

The sources of heat going into and out of the pool are summarized as in Eq. (1). Many of these terms are functions of pool temperature. The pool temperature is calculated using the Newton-Raphson iterative method. One starts with an initial root and proceeds until a certain convergence criterion is met. In the new model, that criterion will be met when the calculated temperature is within 0.1 K of the previous temperature. The initial root is set equal to the boiling temperature of the chemical or the ground temperature, whichever is lower. The ground temperature can be taken to be equal to the air temperature unless other information is available.

The equations of the new evaporation model are generally valid between the freezing point and the boiling point of the chemical. If the calculated temperature drops below the freezing point of the chemical, the pool temperature is set equal to the freezing temperature.⁹ The evaporation rate is then calculated using Eq. (40). This will give a conservative estimate of the evaporation rate.

If the calculated pool temperature is greater than or equal to the boiling point temperature, the pool temperature is set equal to the boiling point temperature. The liquid in the pool will not attain a temperature higher than the boiling point at normal atmospheric pressures. The calculated saturation vapor pressure will be about 1 atmosphere at the boiling point, but may not be exactly 1 atmosphere. To avoid problems such as calculating a chemical mole fraction greater than 1, an alternate equation is used to calculate the boiling temperature evaporation rate [Eq. (3)]:

$$E = \frac{(\dot{Q}_{sol} + \dot{Q}_{atm} - \dot{Q}_{pool} + \dot{Q}_{he} + \dot{Q}_{gd}) A}{H_v}, \text{ kg/s.} \quad (60)$$

where H_v is the heat of vaporization.

3.7 Chemical Data Base

Chemical data for the new model calculations are stored in a data file separate from the program. The six chemical compounds included in the new evaporation model data base are listed in Table 4 along with their chemical formulas and any abbreviations used. With the exception of the hydrazines, most of the physical and thermodynamic data and calculations were taken from the ADAM model data base. The saturation vapor pressure is calculated using the Antoine equation for the non-hydrazine chemicals. This data was obtained from "Lange's Handbook of Chemistry,"¹⁶

Table 4. Chemicals in New Evaporation Model Data Base.

Name	Formula	Abbreviation
Nitrogen Tetroxide	N_2O_4	-
Hydrazine	N_2H_4	-
Monomethylhydrazine	H_2NNHCH_3	MMH
Unsymmetrical Dimethylhydrazine	$(CH_3)_2N-NH_2$	UDMH
Sulfur Dioxide	SO_2	-
Phosgene	$COCl_2$	-

Data and thermodynamic calculations for the hydrazines were obtained from a variety of sources. Data for molecular weight, boiling and freezing temperatures, liquid thermal conductivity, and saturation vapor pressure were obtained from Schmidt,²⁵ a reference devoted exclusively to hydrazine and its derivatives. Vapor viscosity was estimated by the method given in the modified Ille and Springer model at 298 K. A single temperature estimate was made because of the dissimilarity of the calculation to the vapor viscosity calculation in the new model and the lack of data for the hydrazines. Data for the vapor heat capacity and heat of vaporization calculations were likewise taken from the modified Ille and Springer model. Data for the vapor thermal conductivity calculation was found only for hydrazine in Reid et al.²⁴ A constant vapor thermal conductivity of $0.015 \text{ J m}^{-1} \text{ s}^{-1} \text{ K}^{-1}$ is included in the data base for MMH and UDMH. This number was chosen based on the thermal conductivity of hydrazine and some organic compounds at 298 K. Users of the new model should be aware that this is only an estimate to be used until such data becomes available. Thermodynamic equations are valid over a limited temperature range. If a temperature range was not

²⁵ Schmidt, E.W. (1984) *Hydrazine and Its Derivatives: Preparation, Properties, and Applications*, John Wiley and Sons, New York.

available, the freezing point and boiling points are used as the lower and upper bounds of the range of valid temperatures.

4. NEW MODEL SENSITIVITY STUDIES

In the previous sections, a new evaporation model was developed based on the evaluation of three existing evaporation models - the modified Ille and Springer model, the ADAM model, and the Kawamura and MacKay model. In this section, sensitivity studies of the new model are presented in support of the recommendations of the previous sections.

Parameters in the new model are changed one at a time from a set of default parameters to observe the effect on calculated evaporation rate. For instance, the solar radiation calculations from each of the other models will be substituted into the new model to see how they affect the results. Default parameters are listed in Table 5. If conditions are listed as cloudy or "clouds", this means that there is 100 percent cloud cover by low clouds (transmissivity = 0.17). Day refers to 12 noon, and night refers to 12 midnight.

Table 5. Default Values of Parameters for Sensitivity Studies.

Chemical	Nitrogen Tetroxide
Initial Pool Temperature	290 K
Air Temperature	290 K
Ground Temperature	290 K
10 m Wind Speed	4 m/s
Month	4
Day	20
Time - Day	12:00
Time - Night	24:00
Volume Spilled	22 m ³
Average Depth of Pool	1 cm
Cloud Cover Fraction	0 (no clouds) or 1 (clouds)
Cloud Type (for clouds = 1)	Low Clouds
Type of Terrain	Sparse Woods
Ground Type	Wet Soil

4.1 Solar Altitude Angle

In Table 1, it was shown that the differences between calculated solar angles for the ADAM and the Kawamura and MacKay models are trivial (less than 0.5 degree). A worst case scenario is examined in Table 6, which shows that differences in solar altitude angle as high as 5 percent make a difference in the calculated evaporation rate of around 1 percent. Therefore, the selection of the ADAM model solar angle calculation, which was made based on the convenience of the calculation, does not bias the results.

Table 6. Effect of Solar Altitude Angle on Evaporation Rate.

Solar Altitude Angle	Temperature of Pool, K	Evaporation Rate kg/s
60	264.4	9.9
63	264.5	10.0
66	264.6	10.1
69	264.7	10.2
72	264.8	10.3

4.2 Net Heat From Solar Radiation

Comparisons of the three calculation methods discussed in Section 2.1 are shown in Table 7. As expected, the different solar radiation calculations yield the same evaporation rates for nighttime. The ADAM model calculation was incorporated into the new evaporation model because it was the only solar radiation calculation to account for both amount and thickness (transmissivity) of the cloud cover. Table 7 shows that for daytime conditions, both amount and type of cloud cover have some effect on the calculated equilibrium pool temperature and evaporation rate. While that effect is quite small, especially for cloud thickness, it is still reasonable to use the ADAM model solar heating calculation in the new model. The evaporation rates of the new model were most similar to those calculated using the Kawamura and MacKay solar radiation. While it looks as though the modified Ille and Springer model solar radiation does not depend on cloud cover, the evaporation rates are identical as a result of stopping the calculation when it reaches the freezing point.

Table 7. Comparison of Methods for Calculating Net Heat from Solar Radiation.

Source of Solar Radiation Calculation			
Evaporation Rates, kg/s			
Conditions	ADAM (and New Model)	Kawamura and MacKay	Modified Ille and Springer
Day, No clouds	9.9	10.0	8.4
Day, 50% low clouds	9.6	9.2	8.4
Day, 100% low clouds	8.4	8.4	8.4
Day, 100% high clouds	8.6	8.4	8.4
Night, No clouds	2.3	2.3	2.3
Night, 100% low clouds	5.3	5.3	5.3

4.3 Long Wavelength Radiation Emitted by the Atmosphere

The new model was run using a variety of input conditions for atmosphere emissivities of 0.75 and 0.81 (Table 8). These represent a reasonable range of emissivities, as shown in Section 2.2. In all cases, the difference in emissivity produced an insignificant (< 3 percent) change in the calculated evaporation rate. Therefore, the choice of 0.75 for the new model atmosphere emissivity is reasonable.

Table 8. Calculations for Ille and Springer Atmosphere Emissivity (0.75) vs Kawamura and MacKay Atmosphere Emissivity (0.81).

Conditions	Atmosphere Emissivity = 0.75		Atmosphere Emissivity = 0.81	
	Temperature of Pool, K	Evaporation Rate, kg/s	Temperature of Pool, K	Evaporation Rate, kg/s
Day, No Clouds	264.3	9.9	264.5	10.0
Night, No Clouds	276.5	2.3	276.8	2.3
Day, Clouds	262.0	8.4	262.0	8.4
Night, Clouds	263.5	5.3	263.7	5.4

4.4 Long Wavelength Radiation Emitted by the Pool

The emissivity of water ranges from 0.95 to 0.963 (Reference 12). The Ille and Springer, and ADAM models use pool emissivities of 0.95 while the Kawamura and MacKay model uses a pool emissivity of 0.97. Calculated evaporation rate is not expected to vary appreciably over this narrow range of pool emissivity values. As Table 9 shows, the difference in pool emissivity yields a negligible change in the calculated evaporation rate. Therefore, the choice of 0.95 for the new model atmosphere emissivity is reasonable.

Table 9. Calculations for Ille and Springer Pool Emissivity (0.95) vs Kawamura and MacKay Pool Emissivity (0.97).

Conditions	Pool Emissivity = 0.95		Pool Emissivity = 0.97	
	Temperature of Pool, K	Evaporation Rate, kg/s	Temperature of Pool, K	Evaporation Rate, kg/s
Day, No Clouds	264.3	9.9	264.5	9.9
Night, No Clouds	276.5	2.3	276.3	2.2
Day, Clouds	262.0	8.4	262.0	8.4
Night, Clouds	263.5	5.3	263.4	5.3

4.5 Heat Conducted from the Ground

A feature of the new evaporation model is an option to choose the ground or spill surface material. Previous models assumed a ground/surface material and associated thermal properties. Table 10 shows the effect on the pool temperature and evaporation rate of varying the input ground material. During the daytime, ground material makes little difference because other energy exchanges dominate. However, during the night, heat conduction from the ground becomes more important, so the choice of ground material has a significant effect on calculated evaporation rate. For the default nighttime conditions considered here, evaporation rate ranged from 0.9 to 2.3 kg/s for a 2200 square meter spill.

Table 10. Effect of Ground Type on Evaporation Rate.

Ground Type	Daytime - No Clouds		Nighttime - No Clouds	
	Temperature of Pool, K	Evaporation Rate, kg/s	Temperature of Pool, K	Evaporation Rate, kg/s
Dry Soil	262.0	8.4	268.3	1.2
Wet Soil	264.3	9.9	276.5	2.3
Dry Sand	262.0	8.4	263.9	0.9
Wet Sand	262.0	8.4	269.6	1.4
Concrete	262.0	8.4	270.4	1.4

In Section 2.4 a discrepancy between the Kawamura and MacKay and the ADAM heat conduction coefficient was presented. It was concluded that heat conduction from the ground is best estimated from the equation for heat conduction in a semi-infinite solid,¹³ as in the ADAM model. In Table 11, a comparison of the new model and the Kawamura and MacKay model shows that at night the heat conduction from the ground is significant enough that halving the value for the heat conduction coefficient can decrease the calculated evaporation rate by as much as 1/3.

Table 11. ADAM Ground Heat Transfer Coefficient (ADAM h_{grd}) vs Kawamura and MacKay Ground Heat Transfer Coefficient (KM h_{grd}).

Conditions	ADAM h_{grd}		KM h_{grd}	
	Temperature of Pool, K	Evaporation Rate, kg/s	Temperature of Pool, K	Evaporation Rate, kg/s
Day, No Clouds	264.3	9.9	267.5	12.5
Night, No Clouds	276.5	2.3	280.2	3.0
Day, Clouds	262.0	8.4	264.6	10.1
Night, Clouds	263.5	5.3	268.4	7.5

In Section 2.4 it was shown that thermal resistance of the liquid as calculated by the Kawamura and MacKay method is non-negligible compared with the heat conduction through a semi-infinite solid (that is, the ground). At an average pool depth of 0.5 cm, the liquid thermal resistance lowers the overall heat conduction coefficient by 7 percent. As shown in Table 12, this changes the evaporation rate no more than 3 percent. However, for a 2.5 cm average pool depth (5 cm initial depth), the liquid thermal resistance decreases the calculated evaporation rate by as much as 14 percent. The only additional information required to calculate the liquid thermal resistance is the chemical boiling temperature and the liquid thermal conductivity. There are methods available for estimating liquid thermal conductivity, usually from reduced temperature.²⁴

Table 12. Thermal Conductivity of the Ground: Ground and Liquid Thermal Resistance vs Ground Thermal Resistance Only.

Conditions (Initial Pool Depth)	$h_1 + h_g$		h_g Only	
	Temperature of Pool, K	Evaporation Rate, kg/s	Temperature of Pool, K	Evaporation Rate, kg/s
Day, No Clouds (1 cm)	264.3	9.9	264.3	10.1
Night, No Clouds (1 cm)	276.5	2.3	276.9	2.3
Day, Clouds (1 cm)	262.0	8.4	262.0	8.4
Night, Clouds (1 cm)	263.5	5.3	264.9	5.5
Day, No Clouds (5 cm)	262.3	1.9	233.5	2.1
Night, No Clouds (5 cm)	273.9	0.45	275.6	0.52
Day, Clouds (5 cm)	262.0	1.9	262.0	1.9
Night, Clouds (5 cm)	262.0	1.1	262.9	1.2

4.6 Heat Loss Due to Evaporation

4.6.1 PROPERTIES OF VAPOR ABOVE POOL

The new evaporation model uses properties of the chemical vapor/air mixture rather than properties of the pure chemical vapor (as in the ADAM model) or pure air (as in the Kawamura and MacKay model). The consequences of this decision are shown in Table 13. Evaporation rates calculated from using pure chemical properties can be more than twice the evaporation rates of the chemical/air mixture. The evaporation rates calculated from assuming the vapor above the pool is pure air are somewhat lower than the evaporation rates for the mixture. As one does not know *a priori* whether air or chemical will dominate at equilibrium, it is important to use properties of the chemical/air mixture in the calculations.

Table 13. Evaporation Rates Calculated for Chemical/Air Mixture vs Air Only vs Pure Chemical Only.

Conditions	Evaporation Rates, kg/s		
	Chemical/Air Mixture	Pure Air	Pure Chemical
Day, No Clouds	9.9	8.7	17.4
Night, No Clouds	2.3	1.6	3.0
Day, Clouds	8.4	6.4	17.4
Night, Clouds	5.3	4.5	9.9

In the new model, the chemical vapor mole fraction is computed by dividing the saturation vapor pressure at each iteration by the atmospheric pressure. The Ille and Springer model computes an average mole fraction by dividing this value by 2. Table 14 shows the sensitivity of the mole fraction calculation. Dividing the instantaneous value by 2 has the effect of reducing the calculated evaporation rate by 6 percent to 13 percent.

Table 14. Sensitivity of Pure Chemical Mole Fraction (MF) Calculation.

Conditions	$MF = \frac{P_{sat}}{P_{atm}}$		$MF = \frac{P_{sat}}{2P_{atm}}$	
	Temperature of Pool, K	Evaporation Rate, kg/s	Temperature of Pool, K	Evaporation Rate, kg/s
Day, No Clouds	264.3	9.9	265.7	9.4
Night, No Clouds	276.5	2.3	277.9	2.0
Day, Clouds	262.0	8.4	262.0	7.3
Night, Clouds	263.5	5.3	264.6	5.0

4.6.2 MASS TRANSFER COEFFICIENT

The options for calculating the mass transfer coefficient were compared in Section 2.5. The modified Ille and Springer mass transfer coefficient was incorporated into the new model. It accounts for the effect of terrain type and atmospheric stability on the wind profile near the ground through the use of a stability parameter n . Table 15 shows the sensitivity of the stability parameter. The calculated evaporation rate ranges from 3 to 86 kg/s for the default conditions over the range of possible stability parameter values. By contrast, the Kawamura and MacKay model assumes a constant n value of 0.25, which corresponds to an evaporation rate of 17 kg/s for the default conditions.

Table 15. Sensitivity of Stability Parameter n .

n	Temperature of Pool, K	Evaporation Rate, kg/s	Mass Transfer Coefficient, m/s
0.077	262 *	86	0.0494
0.095	262 *	71	0.0407
0.182	262 *	29	0.0110
0.230	262 *	19	0.0107
0.319	264.3	9.9	0.00500
0.333	265.5	9.6	0.00453
0.374	268.6	8.5	0.00343
0.387	269.7	8.3	0.00319
0.400	270.7	8.0	0.00289
0.450	274.5	7.1	0.00213
0.630	286.3	4.7	0.00080
0.675	288.8	4.2	0.00064
0.701	290.3	4.0	0.00056
0.750	292.7	3.5	0.00045
0.797	294.4	3.2	0.00035
1.024	294.4	3.2	0.00045
0.25	262	17	0.00878

* freezing temperature

Table 16 shows evaporation rates calculated using the mass transfer coefficient of the modified Ille and Springer model compared with those calculated using the ADAM model mass transfer coefficient. The stability parameter allows calculation of evaporation rates that differentiate between conditions of day vs night, cloudy vs no clouds, and thick vs sparse vegetation. The ADAM model cannot distinguish between some contrasting conditions.

Table 16. Effect of Mass Transfer Coefficient Calculation on Calculated Evaporation Rate.

Conditions	Mass Transfer Rate Coefficient From:			
	Modified Ille and Springer Model (and New Model)		ADAM Model	
	Mass Transfer Coefficient, m/s	Evaporation Rate, kg/s	Mass Transfer Coefficient, m/s	Evaporation Rate, kg/s
Day, No Clouds, Sparse Woods	0.00502	9.9	0.00498	9.8
Night, No Clouds, Sparse Woods	0.00061	2.3	0.00483	8.4
Day, Clouds, Sparse Woods	0.00483	8.4	0.00483	8.4
Night, Clouds, Sparse Woods	0.00261	5.3	0.00483	8.4
Day, No Clouds, Forest	0.00344	8.5	0.00498	9.8
Day, No Clouds, Grass	0.0407	71	0.00498	9.8
Day, No Clouds, Desert	0.0495	86	0.00498	9.8

Table 17 shows the effect of terrain type on the evaporation rate through the stability parameter. Evaporation rate is very sensitive to the choice of terrain type. Evaporation rates for desert terrain are 4 to 14 times higher than evaporation rates for forest terrain.

Table 17. Effect of Terrain Type on Calculated Evaporation Rate.

Conditions	Type of Terrain			
	Forest	Sparse Woods	Flat/Grass	Desert
Day, No Clouds	8.5 kg/s	9.9 kg/s	71 kg/s	86 kg/s
Night, No Clouds	1.9	2.3	5.1	7.4
Day, Clouds	6.0	8.4	71	86
Night, Clouds	4.3	5.3	19	29

Table 18 shows the effect of wind speed on the evaporation rate, both directly and through the stability parameter [in Eq. (66) for the mass transfer coefficient]. The fact that daytime evaporation rates for 8 m/s winds are lower than those for 4 m/s winds indicates that the stability parameter (which depends on the terrain, sunlight, and wind speed) can actually be more important than the wind speed alone in determining the evaporation rate.

Table 18. Effect of Wind Speed on Calculated Evaporation Rate.

Conditions	Wind Speed			
	1 m/s	4 m/s	8 m/s	12 m/s
Day, No Clouds	7.3	9.9	9.6	10.4
Night, No Clouds	0.36	2.3	7.6	10.0
Day, Clouds	4.8	8.4	7.6	10.0
Night, Clouds	1.5	5.3	7.6	10.0

5. CONCLUSIONS

A new evaporation model has been presented, incorporating elements of several existing evaporation models. The users of the existing models need to know how different the results of their models are from the new model results. Tables 19-21 shows comparisons of calculated evaporation rates from the existing models and the new model. Default values in Table 5 were used.

The Kawamura and MacKay model results shown in Table 19 make less distinction between the day and night conditions than does the new evaporation model. Evaporation rate is directly proportional to the mass transfer coefficient [see Eq. (22)]. However, the mass transfer coefficient in the Kawamura and MacKay model does not include cloud cover or solar angle. Therefore, the evaporation rates calculated by Kawamura and MacKay depend more on calculated temperature and saturation vapor pressure. Terrain type is not used in the Kawamura and MacKay model to calculate the evaporation rate. As indicated by Tables 17 and 19, the Kawamura and MacKay model results are most similar to new model results calculated for sparse woods. The Kawamura and MacKay nighttime evaporation rates are overestimated compared with the new model.

Table 19. Comparison of Kawamura and MacKay Model with New Model.

Time of Day	Cloud Cover %	Cloud Type (New Model Only)	Terrain Type Only	Evap. Rate, kg/s, K&M	Evap. Rate, kg/s, New
Day	0	n/a	Sparse Woods	16.1	9.9
Night	0	n/a	Sparse Woods	13.2	2.3
Day	100	Low	Sparse Woods	14.3	8.4
Night	100	Low	Sparse Woods	13.5	5.3
Day	50	Low	Sparse Woods	15.7	9.6
Day	100	High	Sparse Woods	14.3	8.6

The ADAM evaporation model (just a small part of the ADAM model) yields evaporation rates approximately 2 to 10 times higher than the new evaporation model for conditions shown in Table 20. Furthermore, ADAM evaporation rates vary little from day to night and from cloudy to cloudless conditions. Terrain type is not used in calculating ADAM evaporation rates.

Table 20. Comparison of ADAM Evaporation Model with New Model.

Time of Day	Cloud Cover %	Cloud Type	Terrain Type (New Model Only)	Evap. Rate, kg/s, ADAM	Evap. Rate, kg/s, New
Day	0	n/a	Sparse Woods	24	9.9
Night	0	n/a	Sparse Woods	21	2.3
Day	100	Low	Sparse Woods	22	8.4
Night	100	Low	Sparse Woods	21	5.3
Day	50	Low	Sparse Woods	23	9.6
Day	100	High	Sparse Woods	23	8.6

Table 21. Comparison of Modified Ille and Springer Model with New Model.

Time of Day	Cloud Cover %	Cloud Type (I&S)	Cloud Type (New)	Ceiling, m (I&S)	Terrain Type	Evap. Rate, kg/s, (I&S)	Evap. Rate, kg/s, (New)
Day	0	n/a	n/a	n/a	Sparse Woods	17	9.9
Night	0	n/a	n/a	n/a	Sparse Woods	2.4	2.3
Day	100	Stratus	Low	1000	Sparse Woods	8.4	8.4
Day	100	Stratus	Low	200	Sparse Woods	8.4	8.4
Day	100	Cirrus	High	12000	Sparse Woods	14	8.6
Day	100	Cirrus	High	8000	Sparse Woods	14	8.6
Night	100	n/a	Low	n/a	Sparse Woods	7.2	5.3
Night	100	n/a	High	n/a	Sparse Woods	7.2	5.3
Day	90	n/a	Low	1000	Sparse Woods	14	8.4
Day	90	n/a	Low	200	Sparse Woods	14	8.4
Day	90	n/a	High	12000	Sparse Woods	17	9.0
Day	90	n/a	High	8000	Sparse Woods	17	9.0
Day	50	n/a	Low	n/a	Sparse Woods	17	9.6
Day	50	n/a	High	n/a	Sparse Woods	17	9.8
Day	0	n/a	n/a	n/a	Desert	50	86
Night	0	n/a	n/a	n/a	Desert	9.1	7.4
Day	100	Stratus	Low	1000	Desert	21	86
Day	100	Stratus	Low	200	Desert	21	86
Night	100	n/a	Low	n/a	Desert	20	30

Comparisons of the new model with the Ille and Springer model are shown in Table 21. The new evaporation model is most similar to the modified Ille and Springer model. These are the only evaporation models presented which use the stability parameter to estimate the effect of the wind profile. A drawback of the modified Ille and Springer model is that when cloud cover is less than 100 percent and the ceiling is greater than 4878 m, or when the cloud cover is ≤ 50 percent, the model calculates the same evaporation rate as for no cloud cover. The modified Ille and Springer model does not consider cloud type when cloud cover is less than 100 percent, but it does allow selection of a ceiling height, which is related to cloud type. It also considers terrain type, as indicated by the difference between sparse woods and desert terrain. The modified Ille and Springer model yields higher evaporation rates than the new model for the sparse woods terrain. It yields mostly lower evaporation rates than the new model for desert terrain. In general, the new model yields a greater distinction between cloud conditions and terrain types.

The new evaporation model presented in this report is a composite of existing steady state evaporation models, and is an improvement upon existing models. The model is simple enough to run on a PC, but is complex enough to require a substantial amount of chemical data.

To put the model results into perspective, it is worth noting some of its shortcomings. The new model assumes that the spill surface is flat and impermeable. That is unlikely to be the case, unless the spill surface is concrete. The spill is assumed to be instantaneous, which is not always true. The spill surface area is assumed to be constant, and an average uniform depth is assumed. Again, these are unlikely to hold true in a real spill. In calculating the heat due to solar radiation, a constant pool albedo is assumed. In reality, the albedo of the pool will vary with solar angle. In a spill area with dense vegetation, buildings, or other structures, the pool may be shielded from direct sunlight, even on a cloudless day. Furthermore, season will determine the sparseness of the vegetation. This affects both terrain roughness and solar radiation reaching the pool. The stability parameters used in calculating the mass transfer coefficient are from a single reference source, and apply only to rural areas. An independent verification of these data would place greater confidence in them.

The new model does not consider temperature changes once the temperature is greater than the boiling point or less than the freezing point. It is unlikely that the liquid chemical temperature will exceed the boiling point at ambient pressures. However, the temperature could continue to decrease once the pool has frozen. A number of factors are affected if the chemical freezes and falls below the freezing point. The heat of sublimation (rather than the heat of vaporization) would be required to calculate the evaporation rate. The ground thermal properties may change if the ground is also frozen. The thermal resistance of the pool itself will change when it becomes a solid. Both of these affect the heat conducted from the ground. The albedo of a frozen pool is much higher than that of a liquid pool, so the amount of direct solar heating would be less than for a liquid. The vapor pressure equation is generally not valid for a solid. A temperature-vapor pressure relationship for the solid chemical would be required.

References

1. Kunkel, B.A. (1983) *A Comparison of Evaporative Source Strength Models for Toxic Chemical Spills*, AFGL-TR-83-0307, ADA 139431.
2. Ille, G. and Springer, C. (1978) *The Evaporation and Dispersion of Hydrazine Propellants from Ground Spills*, CEEDO-TR-78-30, ADA 059407.
3. Raj, P.K. and Morris, J.A. (1987) *Source Characterization and Heavy Gas Dispersion Models for Reactive Chemicals*, AFGL-TR-88-0003 (I), ADA 200121.
4. Kawamura, P.I. and MacKay, D. (1987) The evaporation of volatile liquids, *Journal of Hazardous Materials*, 15:343-364.
5. Woolf, H.M. (1980) *On the Computation of Solar Elevation Angles and the Determination of Sunrise and Sunset Times*, National Meteorological Center, Environmental Science Services Administration, Hillcrest Heights, MO.
6. Lunde, P.J. (1980) *Solar Thermal Engineering*, John Wiley and Sons, New York.
7. MacKay, D. and Matsugu, R.S. (1973) Evaporation rates of liquid hydrocarbon spills on land and water, *The Can. J. Ch. Eng.*, 51:434-439.
8. Kunkel, B.A. (1988) *User's Guide for the Air Force Toxic Chemical Dispersion Model (AFTOX)*, AFGL-TR-88-0009, ADA 199096.
9. Holtslag, A.A.M. and Van Ulden, A.P. (1983) A simple scheme for daytime estimates of the surface fluxes from routine weather data, *J. Climate Appl. Meteorol.*, 22:517-529.
10. Kasten, F. and Czeplak, G. (1980) Solar and terrestrial radiation dependent on the amount and type of cloud, *Solar Energy*, 24:177-189.
11. Raphael, J.M. (1962) Prediction of temperature in rivers and reservoirs, *Proc. Amer. Soc. Civ. Eng. J. Power Div.*, 88:PO2.

12. McAdams, W.H. (1954) *Heat Transmission*, 3rd edn., McGraw-Hill Book Company, Inc., New York.
13. Holman, J.P. (1976) *Heat Transfer*, 4th edn., McGraw-Hill Book Company, Inc., New York.
14. Bird, R.B., Stewart, W.E., and Lightfoot, E.N. (1960) *Transport Phenomena*, John Wiley and Sons, Inc., New York.
15. Schneider, P.J. (1955) *Conduction Heat Transfer*, Addison-Wesley Publishing Co., Cambridge, MA.
16. Dean, J.A. (1985) ed. *Lange's Handbook of Chemistry*, 13th edn., McGraw-Hill Book Company, New York.
17. Kothandaraman, C.P. and Subramanyan, S. (1975) *Heat and Mass Transfer Data Book*, 2nd edn., John Wiley and Sons, New York.
18. Sutton, O.G. (1953) *Micrometeorology*, McGraw-Hill Book Company, Inc., New York.
19. Smedman-Hogstrom, A.S. and Hogstrom, U. (1978) A practical method for determining wind frequency distribution for the lowest 200 m from routine meteorological data, *J. of Appl. Meteorol.*, 17:942-954.
20. Fuller, E.N. and Giddings, J.C. (1965) A comparison of methods for predicting gaseous diffusion coefficients, *J. Gas Chromatogr.*, 3:222-227.
21. Fuller, E.N., Ensley, K., and Giddings, J.C. (1969) Diffusion of halogenated hydrocarbons in helium: The effect of structure on collision cross sections, *J. Phys. Chem.*, 73:3679-3685.
22. Fuller, E.N., Schlettler, P.D., and Giddings, J.C. (1966) A new method for prediction of binary gas-phase diffusion coefficients, *Ind. Eng. Chem.*, 58:18-27.
23. Perry, R.H., and Chilton, C.H., eds. (1973) *Chemical Engineers' Handbook*, 5th edn., McGraw-Hill Book Company, Inc., New York.
24. Reid, R.C., Prausnitz, J.M., and Poling, B.E. (1987) *The Properties of Gases and Liquids*, 4th edn., McGraw-Hill Book Company, Inc., New York.
25. Schmidt, E.W. (1984) *Hydrazine and Its Derivatives: Preparation, Properties, and Applications*, John Wiley and Sons, New York.